Jianjun Li (Orcid ID: 0000-0002-3485-5379)
Yueshe Wang (Orcid ID:0000-0003-1767-3175)

Closure Study on Hygroscopic Properties of Water-soluble Matter in Atmospheric $PM_{2.5}$ at a Rural Site in Northwest China

Yukun Chen[1,2], Jianjun Li[2,*], Yueshe Wang[1,*], Xin Wang[1], Gehui Wang[3], Jin Li[2], Can Wu[3],and Lang Liu[2]

[1] State Key Laboratory of Multiphase Flow in Power Engineering, Xi'an Jiaotong University, Xi'an 710049, China;
[2] State Key Laboratory of Loess and Quaternary Geology, Key Lab of Aerosol Chemistry and Physics, Institute of Earth Environment, Chinese Academy of Sciences, Xi'an 710061, China
[3] Key Laboratory of Geographic Information Science of the Ministry of Education, School of Geographic Sciences, East China Normal University, Shanghai 200241, China

*Corresponding authors:
Associate Prof. Jianjun Li
Institute of Earth Environment, Chinese Academy of Sciences, Xi'an 710061, China
Phone: 86-29-6233-6273
Fax: 86-29-6233-6234
Email: lijj@ieecas.cn;

Prof. Yueshe Wang
State Key Laboratory of Multiphase Flow in Power Engineering, Xi'an Jiaotong University, Xi'an, China;
Phone: +86-29-82667323
Mobille: +86-13772023899
Email: wangys@mail.xjtu.edu.cn

Key points:

- Inorganic matters promote the hygroscopicity of particulate matter in summer, while the contribution from organics increases in winter.
- The concentration of sulphate, nitrate, ammonium is higher on heavily polluted days, and the organic matter is high in non-polluting days.
- The rural site of Guanzhong Basin is affected highly by biomass combustion.

Abstract:

In this study, we investigated the chemical composition and hygroscopicity of water-soluble fraction in $PM_{2.5}$ collected from a rural site of Guanzhong Basin, a highly polluted region in northwest China. Hygroscopic growth factors, g(RH), of water-soluble matter(WSM) were measured by hygroscopic tandem differential mobility analyzer(H-TDMA) with an initial dry particle diameter of 100 nm. The $g(90)_{WSM}$ and κ_{WSM} was in the range of 1.08~1.49(1.35±0.10) and 0.04~0.29(0.19±0.06) in summer, 1.24~1.45(1.36±0.07) and 0.12~0.26(0.20±0.05) in winter, respectively. We found that increased nitrate concentration at night in summer suppressed 60-70% of the deliquescent point, and increased g(RH) at elevated relative humidity, compared to daytime. Secondary inorganic ions were the main components in heavy haze day, and greatly contributed to the hygroscopicity of particles. In contrast, more potassium compound and WSOM existed during Chinese Spring Festival event but exhibited no deliquescence point in the process of hygroscopic growth with the elevated RH. The $g(90)_{WSOM}$ and κ_{WSOM}, obtained using ZSR model, were in the range of 1.06~1.52(1.25±0.14) and 0.02~0.32(0.13±0.09) in summer, 1.06~1.58(1.38±0.15) and 0.02~0.38(0.22±0.10) in winter, respectively. The mean $g(90)_{WSOM}$ was in the range of that of biomass burning aerosols, and a good correlation (R=0.71) was found between $g(90)_{WSOM}$ and levoglucosan, confirming that the aerosol's hygroscopicity were highly influenced by biomass burning in winter. Briefly, it is revealed that the aerosol in rural regions of Guanzhong Basin is mainly influenced by biomass burning based on the

hygroscopicity in winter and summer.

Plain Language Summary:

This manuscript reports the chemical compositions and hygroscopic properties of water-soluble fraction in PM2.5 collected from a rural site of Guanzhong Basin, a highly polluted region in northwest China. We found that inorganic components (ammonium and sulphate, etc) are the main substances that promote the hygroscopic properties of particulate matter in summer, while in winter, the contribution from organic matters increases. The SNA concentration is higher on heavily polluted days, and the content of organic matter is high in non-polluting days. The $g(90)_{WSM}$ values measured by H-TDMA and the retrieved κ_{WSM} was in the range of 1.08~1.49(1.35±0.10) and 0.04~0.29(0.19±0.06) in summer, 1.24~1.45(1.36±0.07) and 0.12~0.26(0.20±0.04) in winter, respectively, which is particularly similar to the hygroscopicity parameters of particulate matter produced by biomass burning. We further infer that this region area is affected by biomass combustion due to the fact that the hygroscopicity parameters of WSOM, calculated by E-AIM and ZSR model, is almost equal to the value of the biomass combustion indicator.

1 Introduction

Air quality problems caused by atmospheric particulate matter (PM) is a major concern globally. Research on atmospheric PM has increased over the past decades because of its impact on human health (Brook et al., 2010; Fernández-Camacho et al., 2016; Karagulian et al., 2015; Petrowski et al., 2019), ecosystems and climate change (He et al., 2019; IPCC, 2001; Paraskevopoulou et al., 2015; Zhao et al., 2017). Hygroscopicity, which describes water uptake ability by particles in response to elevated relative humidity(RH) (Alonso-Blanco et al., 2019; Gasparini et al., 2004), is an important thermal dynamic property of atmospheric particles. Due to water ab/adsorption, the particles extinction index will change, the mass and volume will increase and can provide media for heterogeneous chemical reactions(X G Liu et al., 2010; Y Liu et al., 2016b; Y Wu et al., 2017a). The hygroscopicity of particles largely depends on chemical composition, including some water-soluble inorganic matters (WSIM) such as SO_4^{2-}, NO_3^-, and NH_4^+(Junji et al., 2009) and organic matters (WSOM) (J C Zhang et al., 2011a). Another concern is that because the fine $PM_{2.5}$ aerosol particles in the atmosphere contain a variety of components, some of which are highly hygroscopic, the haze events caused by them have become a common weather phenomenon in heavily polluted areas(Ma et al., 2012).

High $PM_{2.5}$ levels can be caused by direct emissions or by the formation of secondary aerosols; the latter are produced from gaseous precursors, especially sulfur dioxide (SO_2), nitrogen oxides (NO_x), ammonia (NH_3), and volatile organic compounds (VOCs), which mainly form the components of sulfate, nitrate, ammonium and organic carbon in the particles(Bi et al., 2007; Chan and Yao, 2008; T J Wang et al., 2012). A lot of previous studies had revealed that chemical composition of $PM_{2.5}$ in China varies significantly in different season, which in general has highest concentration in winter and lowest in summer (Z Liu et al., 2014b; S Wang et al., 2015; L Yao and Lu, 2014). For example, *Shen et al.* indicated that spring samples were highlighted by abundance of Ca_2^+, while the secondary aerosol species (NO_3^-, SO_4^{2-}, and NH_4^+) and OC dominated

in summer, autumn, and winter samples from 2006 to 2007 at Xi'an, China.(Shen et al., 2014) Moreover, a pronounced seasonal variation was observed with relatively lower water content in the colder season, indicating that the inorganic salts were mainly crystalline in winter, whereas they were probably dissolved during the rest of the year(Hueglin et al., 2005). These seasonal variations are related to meteorological conditions, emissions and chemical transformations (Z Liu et al., 2014b; S Wang et al., 2015; L Yao and Lu, 2014), and in turn affect the hygroscopic growth factor in each season.

Guanzhong Basin is one of the most heavily polluted regions in the world with an annual concentration of $PM_{2.5}$ on the ground surface more than 80 $\mu g \cdot m^{-3}$ during 2001–2006(van Donkelaar et al., 2010). Compared to other regions in China such as North China Plain, Yangtze River Delta (YRD), Pearl River Delta (PRD) and Sichuan Basin, air quality in Guanzhong Basin is highly affected by the dust-related emissions from the Loess Plateau in the northwest direction, and the relatively stagnant meteorological condition due to the basin topography(Jianjun Li et al., 2011). Not only the air pollution in Guanzhong urban areas such as Xi'an and Weinan City is serious, but also the situation in the surrounding rural areas is very serious, which may be related to the way of obtaining heat energy(Jin et al., 2018), such as biomass burning. Although some studies have paid attention over the past decades to $PM_{2.5}$ chemical composition and hygroscopicity in East and North China(X-C Chen et al., 2017; Johannesson et al., 2007; J Wang et al., 2013; Yu et al., 2018), few studies were conducted in Guanzhong Basin, especially for its rural areas.

In this experiment, summertime and wintertime $PM_{2.5}$ samples were collected in a rural area of Guanzhong Basin. Some chemical compositions and optical properties of the $PM_{2.5}$ samples were reported elsewhere(Jianjun Li et al., 2020). Here, the hygroscopic growth factor of water-soluble matter in winter and summer under high relative humidity (90%) was determined to investigate the seasonal variation of hygroscopic properties of $PM_{2.5}$ in the rural region. We also combined the contribution of WSIM and WSOM to analyze the influences of chemical compositions and source

emissions on the hygroscopicity of $PM_{2.5}$ in the different seasons.

2 Methodology

2.1 Sample collection

The sampling was performed at at a rural background site, Lin Village (109 ° 32 'E, 34 ° 44' N, 354 m a.m.s.l), Weinan city, in the hinterland of the Guanzhong Basin. No obvious point sources of atmospheric pollution were found nearby the sampling site. Detailed information of the sampling campaign was described by Li et al. (Jianjun Li et al., 2020). Briefly, daytime (08:00 - 20:00) and nighttime (20:00 - 08:00 next morning) $PM_{2.5}$ samples were collected on pre-combusted (450°C for 6 h) quartz filters (Whatman QM/A) using a high volume air sampler (TISCH, TE6070DV-BL, 1.13 $m^3 \cdot min^{-1}$) during Aug. 3-23, 2016 (summer) and Jan. 20 – Feb. 1, 2017 (winter). Field blank samples were also collected at the beginning, middle and end of sampling period by mounting blank filters onto the sampler for about 15 min without pumping any air. Before and after sampling, the sample filters were wrapped in aluminum foil and kept in the refrigerator at -5 ℃ to prevent the decomposition and volatilization of substances.

2.2 Hygroscopicity of water-soluble matter

2.2.1 Hygroscopicity Measurement

A square of ~2.6 cm^2 of the sampling filter was cut (corresponding to 813.6 m^3 sampling air) and extracted with ultrapure water under ultrasonication for 1 hour (15 min each, repeated four times). The dissolved solution was filtered through a PTFE syringe membrane filter (millex-GP, 0.22 μm in pore size, Millipore) to remove water-insoluble suspensions. The water-extract in 30 ml was then placed in the atomizer to generate suspended aerosol particles (S K Boreddy et al., 2016). The generated aerosol particles pass through a Nafion dryer (MD-070-12, ¼″, 14±¼″) and a silica gel diffusion dryer (self-made, I.D.100mm, length 650mm) to remove water and leave crystalline substances (RH<5%), which are then charged positive and negative ions by a corona-discharge electrode operated at a high AC voltage by the neutralizer (^{85}Kr, TSI,

2mCi, Model 3077). After that, the charged polydisperse aerosol particles flow (0.3L/min) went through the first differential mobility analyzer (DMA1, TSI model 3081) with the aerosol to sheath flow ratio as 1:10 to select dry particles with the diameter of 100 nm. The monodisperse100 nm aerosol particles are then introduced into the RH conditioner, where RH is controlled between 10%~93%, transferred to humidified DMA2 for measuring the diameter of particles at defaulted RH. Condensation particle counter (CPC, TSI model 3010) is used to count the humidified aerosol particles. All H-TDMA experiments were performed at room temperature of 298 K and atmospheric pressure of 1 atm(S K Boreddy and Kawamura, 2016; S K Boreddy et al., 2016; Michihiro Mochida and Kawamura, 2004b). The system was calibrated every two hours with pure ammonium sulfate particles at 90 % RH to ensure the accuracy of system(H J Liu et al., 2014a).

2.2.2 Hygroscopicity growth factor calculation

Aerosol hygroscopicity is described by the hygroscopic growth factor, g(RH), which is the ratio of the particle diameter at elevated RH relative to that of the initial dry particles (S K Boreddy and Kawamura, 2016; Suresh Kumar Reddy et al., 2014; Swietlicki et al., 2017) and is given by the following equation:

$$g\left(RH\right)=\frac{D_p\left(RH\right)}{D_{dry}} \quad (1)$$

where D_{dry} is the initial dry particle diameter at RH <5% and $D_p(RH)$ is the diameter at an elevated RH. In this study, the hygroscopic growth factor of the water-extract components at RH of 90, i.e. $g(90)_{WSM}$, was measured for all $PM_{2.5}$ samples. Moreover, a total of 8 samples in typical whether were selected to investigate the hygroscopic behaviors at whole RH range of 10%, 20%, 30%, …, 90%, 93%. Investigation of the hygroscopic growth of particles was reduced to analyzing their size distribution spectra measured before and after particle humidification and fitted with a lognormal Gaussian curve.

2.2.3 Kappa and ZSR calculation

According to the Köhler theory, the hygroscopicity parameter, κ, introduced by

193 Petters and Kreidenweiss(Petters and Kreidenweis, 2007), could be used to describe the
194 hygroscopicity of the aerosol particles based on the H-TDMA measured data(Suresh
195 Kumar Reddy et al., 2014; Swietlicki et al., 2017; Z J Wu et al., 2015; Ye et al., 2013).
196 κ is defined according to:

$$\kappa = \frac{\left(g\left(RH\right)^3 - 1\right)\left(1 - a_w\right)}{a_w} \tag{2}$$

197

198 where g(RH) is the measured growth factor using an HTDMA and a_w is the water
199 activity

$$a_w = \frac{RH}{100}\left(\exp\left(\frac{A}{g\left(RH\right)D_0}\right)\right)^{-1} \tag{3}$$

200

201 with

$$A = \frac{4\sigma_{s/a}M_w}{\rho_w RT} \tag{4}$$

202

203 where $\sigma_{s/a}$ is the surface tension of the solution–air interface, M_w is the molar mass of
204 water, ρ_w is the density of water, R is the universal gas constant, T is the temperature
205 in Kelvin, and D_0 is the droplet diameter.

206 Assuming there is no interaction between different components of WSM, GF of
207 internally mixed particles can be reproduced based on the ZSR relation as followed
208 (Luo et al., 2020):

$$g_{mixed} = \left[\sum_i \left(\varepsilon_i g_i\right)\right]^{1/3} \tag{5}$$

209

210 where g_i is the hygroscopic growth factor of species i and ε_i is its volume fraction in the
211 mixed WSM.

212 ## 2.3 Chemical Analysis

213 A punch of the filter sample (~8.6 cm^2) was extracted with Milli-Q water (18.2MΩ),
214 and filtered through a PTFE syringe filter. Then the water-extract was analyzed for
215 water-soluble inorganic ions (SO_4^{2-}, NO_3^-, NH_4^+, Cl^-, Ca^{2+}, K^+, Na^+ and Mg^{2+}) using a
216 Metrohm Ion Chromatography (Metrohm 940, Switzerland) and WSOC using a
217 Shimadzu TOC analyzer (TOC-L CPH, Japan). After every 10 samples are tested, one
218 sample is randomly selected for repeated test. Concentrations of individual molecules,

including levoglusosan, galactosan, and mannosan, were measured using GC/EI-MS (Agilent 7890A-5975C, USA) calibrated by authentic standards. The details for the sample extraction procedures and chemical measurements were provided in previous publications (J. Li et al., 2014; Jianjun Li et al., 2020; Steven et al., 2016; T Zhang et al., 2011b).

3 Result and discussion

3.1 Chemical composition of WSM

Previous studies indicated that the water-extract of atmospheric aerosol is mostly composed of water-soluble inorganic ions, metals, and organic matters (WSOM). However, water-soluble metals were not discussed in this study because their contribution to hygroscopic can be neglected compared with inorganic ions and OM in the extract of atmospheric fine particulate (Swietlicki et al., 2017; H. Xu et al., 2019). What's more, the concentration of WSOM could be calculated by multiplying the concentration of WSOC by a factor of 2.1(Aggarwal et al., 2007; S K Boreddy et al., 2016; Jung et al., 2011). Figure 1 summarizes the temporal variation of mass concentration of $PM_{2.5}$ and each water-soluble matter in both summer and winter. The average mass concentration of $PM_{2.5}$ in winter is about three times higher than that in summer (Figure 1a and Table 1), mainly attributed to enhanced emissions from residential activities for house heating and relatively stable meteorological conditions in winter(Sun et al., 2019; X Zhang et al., 2019). The wintertime $PM_{2.5}$ concentration (185.5μg m^{-3}) in this study is comparable to that in Nanliu Village (191.0 μg m^{-3}), another small village about 110 km away from the Lin Village, in the winter of 2016 (Hongmei Xu et al., 2018), suggesting that $PM_{2.5}$ pollution is regional rather than local in the Guanzhong Basin area.

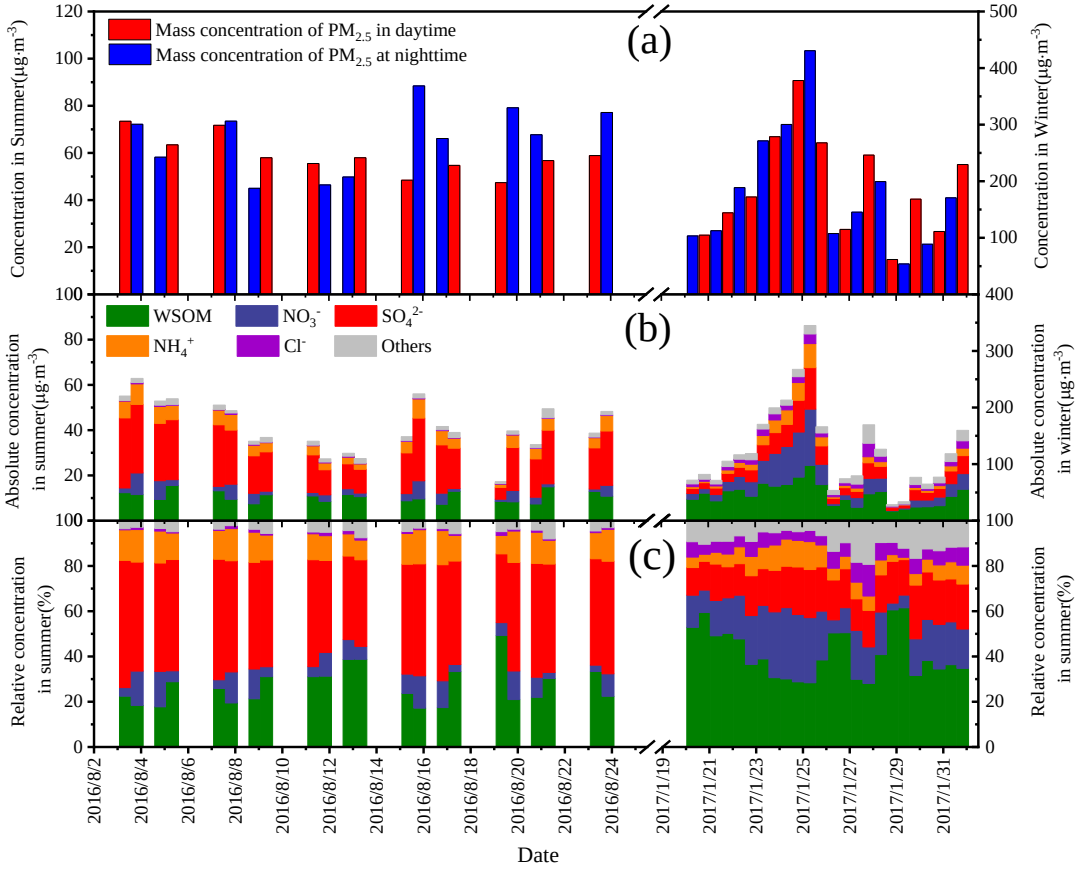

Figure 1 $PM_{2.5}$ concentration and concentration and proportion of water-soluble substances during the two sampling campaigns.

Table 1 Concentration and proportion of water-soluble ions and organic carbon in $PM_{2.5}$

WSM	Summer			Winter		
	Average	Proportion in $PM_{2.5}$	Proportion in WSM	Average	Proportion in $PM_{2.5}$	Proportion in WSM
WSOM	10.63±1.11	17.55%±4.51%	27.04%±8.18%	45.97±9.28	26.72%±7.20%	41.18%±10.64%
NH_4^+	5.31±1.93	8.40%±2.35%	12.40%±1.96%	10.68±10.28	4.71%±2.25%	7.05%±2.90%
Cl^-	0.37±0.11	0.61%±0.20%	0.94%±0.32%	7.56±4.99	3.99%±1.46%	6.15%±2.14%
NO_3^-	3.61±2.49	5.66%±3.54%	8.37%±4.33%	26.93±24.84	12.11%±5.61%	18.04%±7.39%
SO_4^{2-}	19.97±6.66	31.72%±8.33%	46.80%±5.54%	22.52±15.98	11.40%±2.38%	17.48%±2.86%
Other ions	1.79±0.62	2.96%±1.15%	4.45%±1.38%	10.89±5.75	6.46%±2.49%	10.09%±4.10%
Total ions	31.05±10.35	50.11%±13.05%	72.96%±8.18%	78.58±56.60	38.86%±9.43%	58.82±10.64%

The total amount of WSM, i.e. the sum of WSOM and water-soluble inorganic ions, accounts for 66.93% and 67.16% of $PM_{2.5}$ concentration in summer and winter, respectively. Inorganic ions predominate the WSM concentration in both seasons, accounting for more than 50% of WSM. However, the contribution of WSOM to WSM increases by 1.4 times from 27.04±8.18% in summer to 41.18±10.64 % in winter (Table 1). In summer, the high temperature and solar radiation are favorable for atmospheric

photochemistry activity, and thus can enhance the formation of secondary pollutants (Calvo et al., 2008). Thus, the contribution of the sum of NO_3^-, SO_4^{2-}, and NH_4^+ to WSM is always higher than 50% in summer (Figure 1). Sulfate is the most abundant composition, accounting for about half of WSM, followed by decreasing in order of WSOM, NH_4^+, and NO_3^-. In winter, however, WSOM becomes the most abundant composition, accounting for more than one third of WSM in both daytime and nighttime. The contribution of SO_4^{2-}, NO_3^-, and NH_4^+ increased continuously during the haze period(Ge et al., 2019; G Wang et al., 2018a; G Wang et al., 2016a; Xie et al., 2020) (January 23rd to 26th, 2017), because the high RH and stable meteorological condition are favorable for their secondary formation. This result agrees well with most previous studies in China (An et al., 2017; S Y Chen et al., 2015; X Wang et al., 2018b; Xiang et al., 2016; Yue et al., 2015). However, it is worth noticing that the content of Cl^- in the particles is relatively stable, regardless of whether it is haze weather, which may indicate that primary emission changes litter during winter.

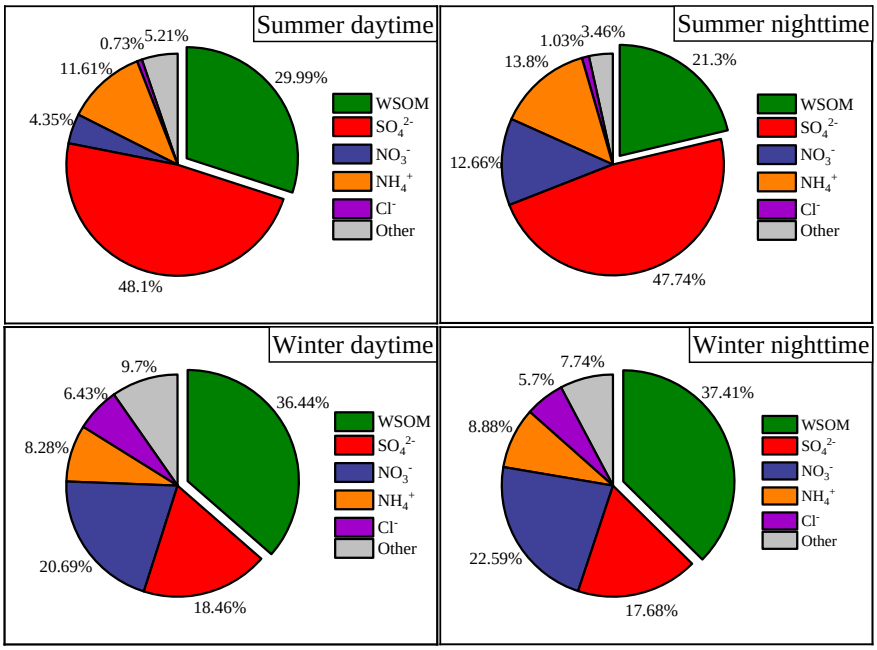

Figure 2 Comparison of water-soluble matters between daytime and nighttime in both seasons.

Figure 2 shows the proportion of day and night components during summer and winter sampling. In summer, the contribution of NO_3^- (12.66%) in nighttime increases by around 3 times compared with that in daytime (4.35%), which is related to the enhancing gas-to-particle partitioning at lower temperature in nighttime. The

proportion of WSOM at nighttime (21.30%) is lower than that in daytime (29.99%), because more secondary OM are formed in daytime. In winter, however, the proportion of water-soluble matters in the samples collected in the daytime and at nighttime has almost no change, which is different from that in summer. And it could also indirectly be explained by the static and stable environmental conditions between day and night in winter.

3.2 Variation of g(90)WSM in association of chemical compositions

Figure 3 shows the temporal variation of $g(90)_{WSM}$ and κ_{WSM} in both seasons. Although the average values of $g(90)_{WSM}$ in summer (1.35±0.10) and winter (1.36±0.07) are comparable, daily $g(90)_{WSM}$ presents an obvious variation in both seasons (1.08~1.49 in summer and 1.24~1.45 in winter). The results indicate that the hygroscopic properties of $PM_{2.5}$ in the region are highly affected by biomass burning. The hygroscopic growth factor also showed a distinct diurnal pattern with higher value at night in summer, while in winter the value of day and night was almost the same, which should be attributed by the different by the proportion of different components in WSM.

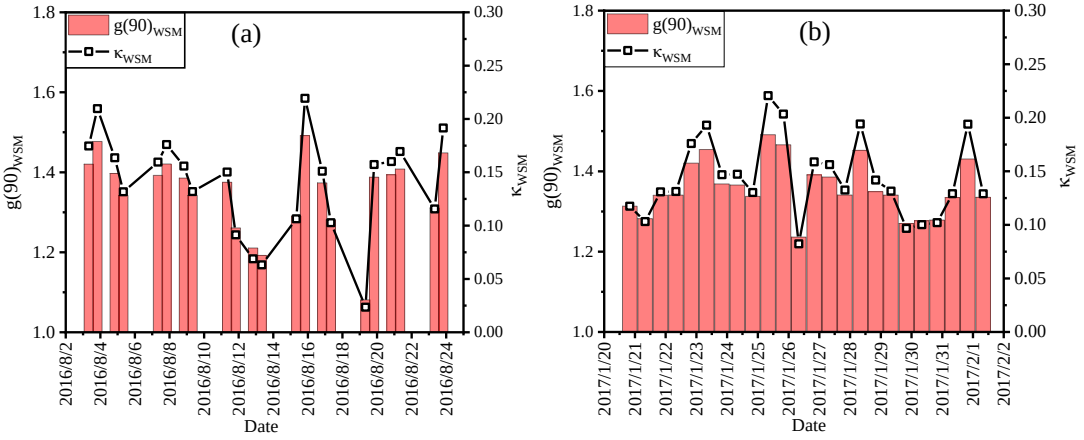

Figure 3 The temporal variation of $g(90)_{WSM}$ and κ_{WSM} in both seasons: (a) for summer, (b) for winter.

The correlation coefficient (R) is 0.71 in summer and 0.50 in winter between $g(90)_{WSM}$ and $PM_{2.5}$, indicating that the particles in summer environment contain more substances that are more hygroscopic (e.g., SO_4^{2-}) than that in winter, as shown in Figure 4(a)(Steven et al., 2016). The linear correlation between $g(90)_{WSM}$ and major

ionic components in different seasons are shown in Figure 4. In summer, $g(90\%)_{WSM}$ presents a strong correlation with sulfate (R=0.86, Figure 4(b) and ammonium (R=0.88, Figure 4(d)), implying that secondary inorganic ions formed from precursors are important for the growth factor of $PM_{2.5}$ over Guanzhong Basin in summer. The nitrate (R^2=0.61, Figure 4(c)) shows a weaker correlation with $g(90\%)_{WSM}$, indicating their weak contribution due to the relatively low abundance. Organic matters seems have neglectable effect to the $g(90\%)_{WSM}$ in summer (R<0.1; p>0.1). The correlations of $g(90\%)_{WSM}$ with inorganic ions are much weaker in winter, e.g., the coefficients (R) is 0.50 for sulfate, 0.49 for nitrate, and 0.50 for ammonium, respectively. These results suggest that the role of inorganic ions playing on the hydroscopic property of WSM of $PM_{2.5}$ decreased in winter. Whereas, the effect of water-soluble organic matter increased slightly so that it also have a weak correlation with $g(90\%)_{WSM}$ (R=0.45, p<0.01; Figure 4(e)) in winter. Moreover, the correlation coefficients (R) between biomass burning tracers, i.e. levoglucosan, galactosan, mannosan, and hygroscopic growth factor of WSM at 90% RH are 0.54 (Figure 4(f)), 0.49, 0.52 (not shown as figures), respectively(S K R Boreddy et al., 2014; Jung et al., 2011; M. Mochida and Kawamura, 2004a). The correlation coefficient of biomass burning indicators is larger than that of WSOM, revealing that the source of biomass burning has a significant contribution to the hygroscopicity of aerosols, and is the major part of organic matter.

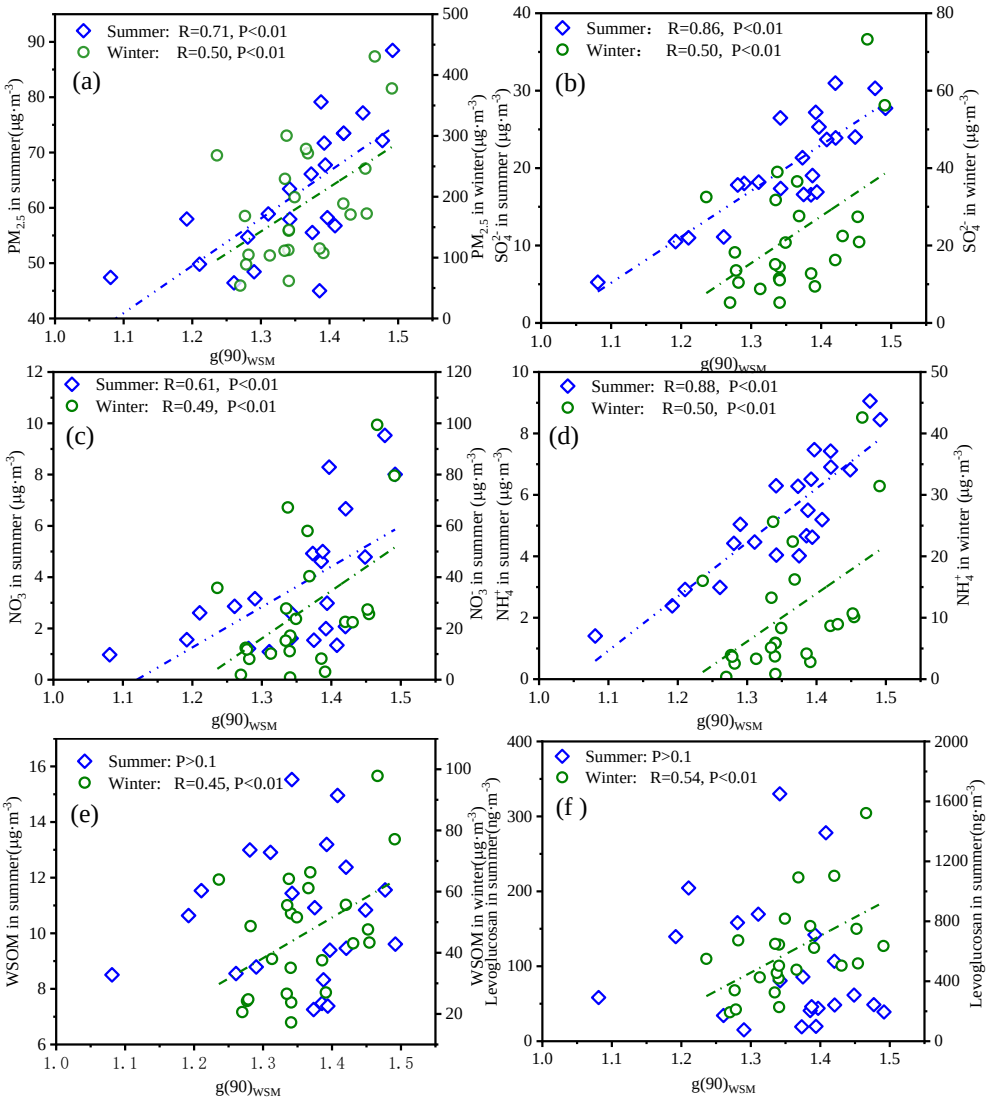

Figure 4 Scatter plots and Linear fit curve between $g(90\%)_{WSM}$ versus mass concentration $PM_{2.5}$ and WSM mass concentration of different chemical species: (a) mass concentration $PM_{2.5}$ in summer,(b) SO_4^{2-}, (c) NO_3^-,(d) NH_4^+, (e) WSOM, (f)levoglucosan in the $PM_{2.5}$ aerosols collected at Lin Village.

κ_{WSM} values derived from hygroscopic growth factor measured by H-TDMA in both seasons are presented in Figure 3. The calculated κ_{WSM} ranges from 0.04~0.29 averaged of 0.19±0.06 in summer and 0.12~0.26 with the average of 0.20±0.05 in winter, respectively. The hygroscopic growth factor of the WSM in the environmental $PM_{2.5}$ aerosol in this study are significantly lower than that of other regions, such as marine sites and urban sites (Table 2). This related to the composition of aerosols in different regions(Y Liu et al., 2016b). Marine aerosols contain a large amount of inorganic salts, of which Na^+ and Cl^- are the most abundant, showing very high hygroscopicity (2.1)(S K Boreddy and Kawamura, 2016; S K Boreddy et al., 2016). In addition, the

hygroscopicity parameters of water-soluble matter in urban environments aerosols are higher than those of rural aerosols due to the influence of sulfate and nitrate discharged by more human activities in urban areas (Y Liu et al., 2016b; Ye et al., 2013; J C Zhang et al., 2011a). At rural and suburban sites, however, $PM_{2.5}$ aerosols contain more water-soluble organic matters(Jin et al., 2018; Suresh Kumar Reddy et al., 2014) with lower hygroscopicity than SNA and NaCl(Swietlicki et al., 2017). In this study, the samples were collected at rural site, Lin village, with the proportion of water-soluble organic matter in winter and summer was 27.04% and 41.18% respectively. Therefore, the measured hygroscopic growth factor with HTDMA is closer to the value of less hygroscopicity, such as biomass burning aerosols, and the value of the retrieved hygroscopicity parameter, κ, is smaller.

Table 2 Hygroscopicity parameters of WSM, κ_{WSM}, extracted from environmental aerosols.

RH	Site	Time	Particles	Instruments	κ_{WSM}/g(RH)$_{WSM}$	Reference
90%	Lin village (109°32'E, 34°44' N)	Aug. 3rd-23rd, 2016 Jan. 20th to Feb. 1st, 2017	$PM_{2.5}$	H-TDMA	0.023-0.219 summer (0.140±0.047) 0.097-0.221 winter (0.144±0.036) (κ_{WSM})	In this study
90%	East China Sea (119°E–126°E, 22°N–35°N)	May 18- June 12, 2014	TSP	H-TDMA	0.46-1.56（0.88 ± 0.35）(κ_{WSM})	(Yan et al., 2017)
90%	Morogoro, Tanzania, in East Africa. (06°47′40.8″S, 37°37′44.5″E)	June–August 2011	$PM_{2.5}$	H-TDMA	0.04-0.24 (0.11±0.07) (κ_{WSM})	(Suresh Kumar Reddy et al., 2014)
90%	Chichijima Island, Japan (27°04′N, 142°13′E)	January–September 2003	TSP	H-TDMA	0.20-0.97 (0.51±0.17) (κ_{WSM})	(S K Boreddy and Kawamura, 2016)
85%	Xi'an (109.1°E,34.23°N)	9th-12th Mar., 2013	TSP	H-TDMA	0.21-0.38 (Most are around 0.3) (κ_{WSM})	(H Yao et al., 2015)
34.22±14.81% **60.17±13.54%** **45.39±17.78%** **30.34±12.07%** **45.61±18.81%**	Beijing (39°59′21″N, 116°18′25″E)	Jan. 16th - Dec. 29th, 2007	$PM_{2.5}$	H-TDMA	0.22±0.13(spring) 0.26±0.08(summer) 0.24±0.07(autumn) 0.25±0.05(winter) 0.25±0.09(annual)	(Y Liu et al., 2016b)
90%	Bay of Bengal, BOB (4°–22°N,76°–98°E)	Dec. 27th, 2008- Jan. 30th, 2009	$PM_{2.5}$	H-TDMA	1.11-1.74 (1.43±0.19) Northern of BOB;	(S K Boreddy et al., 2016)

					1.12-1.38 (1.25±0.09) Southern of BOB; ($g(RH)_{WSM}$)	
85% **90%**	Chichijima Island, Japan (27°04′N; 142°13′E)	2001–2002	TSP	H-TDMA	1.54±0.12 (85%) 1.76±0.11 (90%) ($g(RH)_{WSM}$)	(S K R Boreddy et al., 2014)

Hygroscopicity parameters, κ, is typically characterized in the range of $0.1<\kappa<0.9$ for atmospheric particular(Petters and Kreidenweis, 2007). What's more, biomass-burning aerosols was significantly lower than that of typical urban aerosols (Z J Wu et al., 2015). Previous studies have focused on the biomass burning aerosols typically, which exhibit lower hygroscopic properties and are therefore classified as less-hygroscopic particles(Kreidenweis and Asa-Awuku, 2014). The κ values of biomass-burning aerosols are reported to be 0.05–0.1 in the African savannah (Kotchenruther and Hobbs, 1998), 0.1 in Brazil (Magi and Hobbs, 2003), 0–0.04 for the almost hydrophobic modes and 0.06–0.13 the less hygroscopic modes in Amazonia(Swietlicki et al., 2017), and 0.11±0.07 (range: 0.04–0.24) in Tanzania(Suresh Kumar Reddy et al., 2014), respectively. An average κ of 0.08 for 100 nm particles for freshly emitted particles from the burning of different hard and soft woods(Dusek et al., 2010b), biomass-burning secondary organic aerosols was 0.11(Engelhart et al., 2012), environmental aerosol particles are about 0.1 in Beijing (Z Wu et al., 2017b)and 0.16 ± 0.006 in Athens(Psichoudaki et al., 2018). However, a wider range of hygroscopic parameters of biomass combustion aerosols has also been reported. For examples, the κ values ranging from 0.01 to 0.55 for grass burning are reported by Andreae and Rosenfeld(Andreae and Rosenfeld, 2008), DeMott et al. derived κ values in the range of 0.02–0.56 from H-TDMA data(Demott et al., 2009), and Maria et al. calculated that it is in the range of 0-0.39 for fresh wood combustion particles. Interestingly, the mean of κ_{WSM} (~0.19 in summer and ~0.20 in winter) in this study is comparable to that of biomass burning aerosols measured by Rose et al. with the average κ value elevated to 0.20 during a strong local biomass burning event near the mega-city Guangzhou, China (Rose et al., 2010). In addition, the κ value from crop residues burning ranges from 0.20 to 0.35.(C Li et al., 2016). Therefore, it can be

concluded that $PM_{2.5}$ in this area is greatly affected by biomass combustion emissions according to the correlation between biomass burning indicators and $g(90)_{WSM}$, as well as hygroscopicity parameters.

3.3 Hygroscopic Growth Curves of WSM

Aerosol particles, particularly the water-soluble matter have the ability to ab/desorb water vapor during their interaction in the atmosphere, thus affecting their size, optical properties, and aqueous phase reactions(X G Liu et al., 2010; Y Liu et al., 2016b). Therefore, it is of great significance to explore the hygroscopicity in the atmosphere. To further investigate the hygroscopic growth of WSM in the $PM_{2.5}$ aerosols, four pairs of $PM_{2.5}$ samples in typical weather or event, that are summertime samples (day and night on 3 August, 2016), wintertime severe haze event (day and night on 25 January, 2017), wintertime clean day (day and night on 29 January, 2017), and Chinese Spring Festival event (night on 27 January, 2017 and day on January 28, 2017), were chosen to analyze their hygroscopic growth at RH ranging from 10% to 93%.

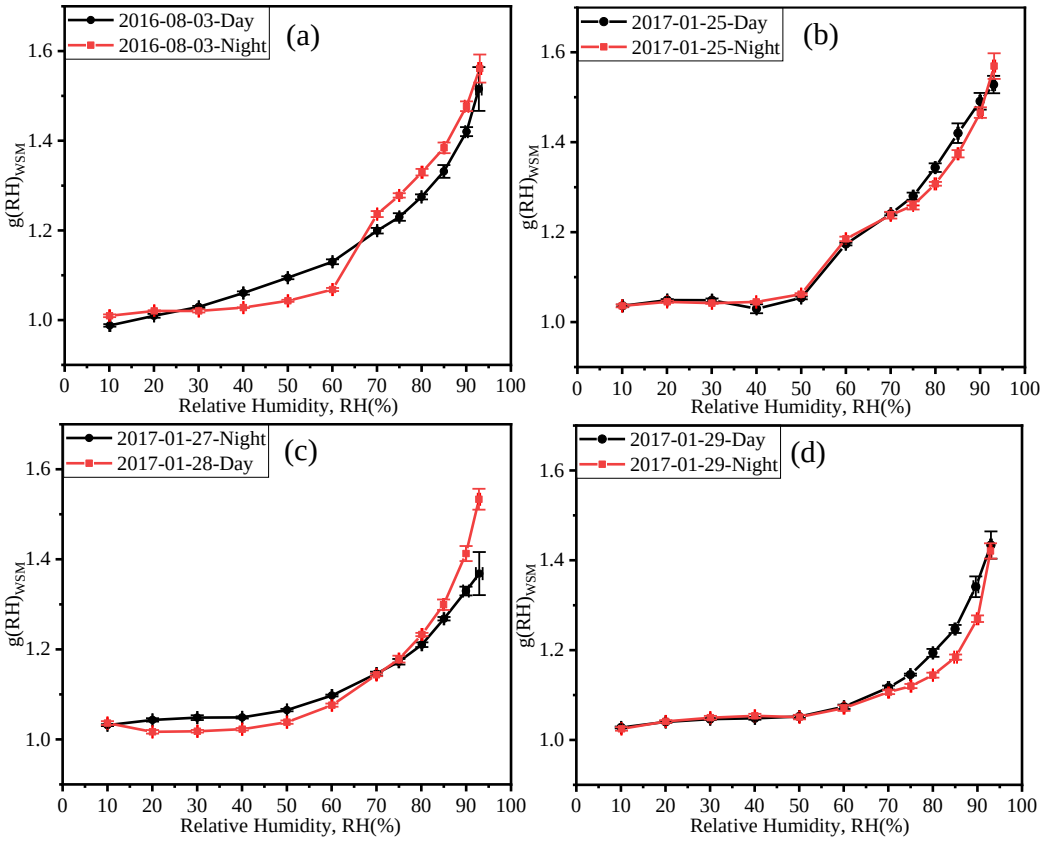

Figure 5 Changes in hygroscopic growth factor of the WSM ($g(RH)_{WSM}$) of aerosol particles nebulized from water extracts of samples, as a function of RH under hydration experiments. (a) for

typical summer weather, (b) for heavy haze day, (c) for the China New year Eve and the first day of the new year, (d) for no-pollution day.

Figure 5 shows the changes in g(RH) of the WSM, as a function of RH under hydration experiments. The hygroscopic growth curve of water-soluble substances in summer has no obvious deliquescence point in the daytime, however, a clear deliquescent point appears between 60%~70% during the night (Figure 5(a)). When the RH is in the range of 30%~60%, the $gfs(RH)_{WSM}$ in daytime are greater than those in nighttime. However, the $gfs(RH)_{WSM}$ in daytime are less than that in nighttime when RH are higher than 60%, which attributed to the distinct organic to inorganic ratios in WSM. As shown in Figure 6(a) and (b), inorganic salts dominated the water-soluble matter in both summertime samples. When the relative concentration of nitrate increases at night, the solution after ab/adsorbing water is more inclined to form the mixed aqueous solution of nitrate and sulfate(Schaap et al., 2004). Therefore, it could be inferred that the deliquescent relative humidity (DRH) is in the range of 60%~70% due to the abrupt increased growth factor. For solutions with more than two electrolytes, the deliquescent relative humidity (DRH) of a salt in a multicomponent solution is always lower than its DRH in solution alone(Wexler and Seinfeld, 1991). In addition, the internal mixing of organic and inorganic aerosol components usually leads to a decrease of deliquescence and efflorescence RH(Mikhailov et al., 2009). Therefore, when the concentration of nitrate increases from day to night with 3.76% to 15.15%, the deliquescence point of mixed electrolyte will be reduced to be closer to that of NH_4NO_3. The first deliquescence point of the NH_4NO_3–$(NH_4)_2SO_4$ system occurs at RH=61.2~61.3%, and the second-stage hygroscopic growth occurs at RH=77~78% when the system becomes a saturated solution droplet(Lee et al., 2001). On the other hand, nitrate during the night showed a substantial increase of about 12%, while the sulfate concentration produced a decrease of about 10%. Thus, increased nitrate concentration can reduce the deliquescent point of the mixed particles(Wexler and Seinfeld, 1991), which is consistent with the results during nighttime of summer in this study. As shown in Figure 6(a) and (b), inorganic salts dominate the water-soluble substance in both summertime samples. WSOM also contributes substantially to WSM

in $PM_{2.5}$, and its concentration is higher during the day-time than at night-time. Previous studies indicated that the organic matters could affect the hygroscopicity of inorganic salts by decreasing the deliquescence point of salt, changing the efflorescence point or suppressing the crystallization of salts(Bouzidi et al., 2020; Q Liu et al., 2016a; Y Wang et al., 2016b; Z Wang et al., 2018c).No obvious deliquescence point was found is mainly because of the higher contribution of WSOM in the daytime(Dusek et al., 2010a; Z Wang et al., 2018c).

In the three typical events of winter, the proportion of inorganic and organic substances has greatly changed. In heavy haze day in winter, the particulate hygroscopic deliquescence point obviously emerges between 50%~60% with the growth factor increase from 1.05 at 50% RH to 1.17 at 60% RH in Figure 5(b). In terms of chemical composition from Figure 6(c) and (d), it can be found that although the proportion of organic matter soluble in water during heavy haze weather is higher than that in summer, the inorganic SNA (sulfate, nitrate, ammonium) is still the main component, which greatly contributes to the hygroscopic properties of particles. In severe haze days, the concentration of nitrate is dominant, followed by sulfate, which is fundamentally different from that in summer. When the relative humidity is below 50%, there is no significant increase in the size of the particles, similar to the characteristics contained in inorganic substances. But after that, the particles grow rapidly and become larger, and the growth factors of particulate matter during the day and nighttime are comparable in each RH condition. This is consistent with the average day and night comparison of the whole process in the previous analysis. During this period, the content of components represented by day and night is almost the same, which also indirectly explain the unfavorable atmospheric photochemistry and low wind speed in the rural area in winter. However, no significant abrupt change in the hygroscopic growth curve of particulate matter were found for clean day (Figure 5(d)) and Chinese Spring Festival event (Figure 5(c)). More potassium matters were emitted from the fireworks and firecrackers on Chinese Spring Festival event. For K_2SO_4, the DRH was reported to be 96%, while KNO_3 displayed continuous hygroscopic growth (Freney et

al., 2009; Tang et al., 2019). Thus, no deliquescence was observed in the samples during the Spring Festival. And the emissions on the first day of the new year are more than New Year's Eve. Unlike daytime, the concentration of nitrate is higher, which is due to the intensification of nitrogen oxides to nitrate during the night. As the no-pollution day is close to the Spring Festival, and the continuous firecracker emissions in rural areas, the proportion of inorganic aerosol components such as potassium and sodium ions is still high. Compared with that in summer typical day, the content of WSOM in environmental particles in winter has been increased significantly. Especially, in clean day, WSOM accounts for about 60% of WSM (Figure 6(g) and (h)). Due to the large proportion of organic matter, the hygroscopic growth factor of WSM with the increase of relative humidity tends to be more consistent with that of organic matter without deliquescence point. In addition, on no-pollution day, the proportion of sulfate in the inorganic component SNA is still the highest except for WSOM, similar to that in summer.

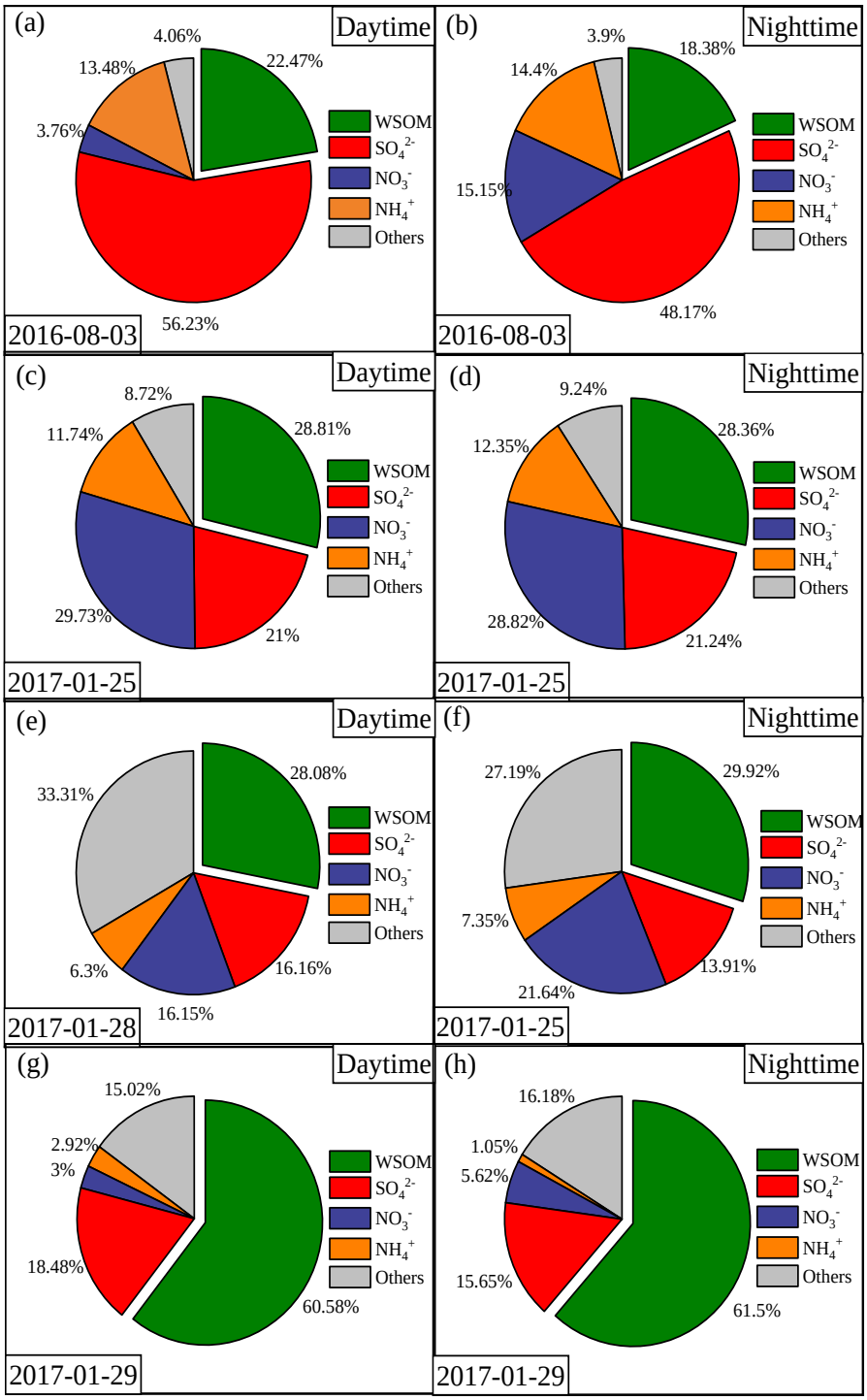

Figure 6 Composition of water-soluble substances in typical weather.

3.4 Hygroscopic Growth of WSOM

Generally, the hygroscopic property of environmental particles is mainly controlled by the inorganic to organic ratios contained in them. The additional water, which cannot be explained by the WSIM, can be then attributed to the WSOM(Jung et al., 2011;

460 Suresh Kumar Reddy et al., 2014). However, the measurement of hygroscopic
461 characteristics of water-soluble organic substances is still insufficient in the currently
462 applicable technology. There are several studies which have confirmed that the use of
463 the ZSR mixing rule can achieve a better chemical composition and particle
464 hygroscopicity closure(Almeida et al., 2019; Dusek et al., 2010a; Meyer et al., 2008).
465 The $g(RH)_{WSOM}$ can be calculated as follows:

466
$$g(RH)_{WSOM} = \left[\frac{g(RH)_{WSM}^3 - \left(\varepsilon_{WSIM}\, g(RH)_{WSIM}\right)^3}{\varepsilon_{WSOM}} \right]^{\frac{1}{3}} \quad (6)$$

467 where ε_{WSIM} and ε_{WSOM} represent the volume fractions of WSIM and WSOM in the
468 WSM, respectively. These two values are listed in Table 3. The $g(RH)_{WSIM}$ corresponds
469 to the growth factor of water-soluble inorganic substance, which are calculated by
470 model IV of E-AIM (S K Boreddy and Kawamura, 2016; Jung et al., 2011; Q Liu et al.,
471 2016a; Suresh Kumar Reddy et al., 2014). K^+, Ca^{2+}, and Mg^{2+} that are not included in
472 the model are converted into equivalent Na^+ based on charge conservation (Hennigan
473 et al., 2015). $g(RH)_{WSIM}$ can be calculated by the Zdanovskii–Stokes–Robinson (ZSR)
474 model according to the chemical compositions of the mixture, which is based on the
475 linear addition of water content of individual component in the mixture(Bouzidi et al.,
476 2020; Jung et al., 2011; Z Wang et al., 2018c). The composition of organic matter causes
477 the density to change, and it is found that the density is mainly distributed near 1.4g/cm^3
478 during measurement(Aggarwal et al., 2007; Dick et al., 2000; Jung et al., 2011)

479 Table 3 Volume fractions of water-soluble inorganic matter (WSIM), water-soluble organic matter
480 (WSOM) and growth factor of water-soluble inorganic matter ($g(90\%)_{WSIM}$)during two campaign

Date	Summer			Date	Winter		
	ε_{WSIM}	ε_{WSOM}	$g(90)_{WSIM}$		ε_{WSIM}	ε_{WSOM}	$g(90)_{WSIM}$
2016/8/3	0.72	0.28	1.82	2017/1/20*	0.38	0.62	2.04
2016/8/3*	0.77	0.23	1.86	2017/1/21	0.30	0.70	2.03
2016/8/4*	0.78	0.22	1.86	2017/1/21*	0.41	0.59	2.00
2016/8/5	0.64	0.36	1.84	2017/1/22	0.40	0.60	2.00
2016/8/7	0.68	0.32	1.83	2017/1/22*	0.44	0.56	1.96
2016/8/7*	0.76	0.24	1.86	2017/1/23	0.55	0.45	1.98
2016/8/8*	0.73	0.27	1.87	2017/1/23*	0.54	0.46	1.99
2016/8/9	0.61	0.39	1.85	2017/1/24	0.63	0.37	1.96

2016/8/11	0.61	0.39	1.84	2017/1/24*	0.64	0.36	1.94
2016/8/11*	0.61	0.39	1.87	2017/1/25	0.65	0.35	1.94
2016/8/12*	0.53	0.47	1.88	2017/1/25*	0.66	0.34	1.94
2016/8/13	0.52	0.48	1.87	2017/1/26	0.54	0.46	1.93
2016/8/15	0.70	0.30	1.84	2017/1/26*	0.38	0.62	2.03
2016/8/15*	0.78	0.22	1.84	2017/1/27	0.40	0.60	2.00
2016/8/16*	0.78	0.22	1.84	2017/1/27*	0.59	0.41	2.02
2016/8/17	0.59	0.41	1.83	2017/1/28	0.62	0.38	2.09
2016/8/19	0.42	0.58	1.87	2017/1/28*	0.50	0.50	2.04
2016/8/19*	0.74	0.26	1.85	2017/1/29	0.29	0.71	2.04
2016/8/20*	0.72	0.28	1.84	2017/1/29*	0.26	0.74	2.07
2016/8/21	0.61	0.39	1.84	2017/1/30	0.58	0.42	2.02
2016/8/23	0.59	0.41	1.83	2017/1/30*	0.52	0.48	1.98
2016/8/23*	0.72	0.28	1.84	2017/1/31	0.56	0.44	1.99
				2017/1/31*	0.54	0.46	1.98
				2017/2/1	0.56	0.44	2.00

* represent particulate matter collected at night.

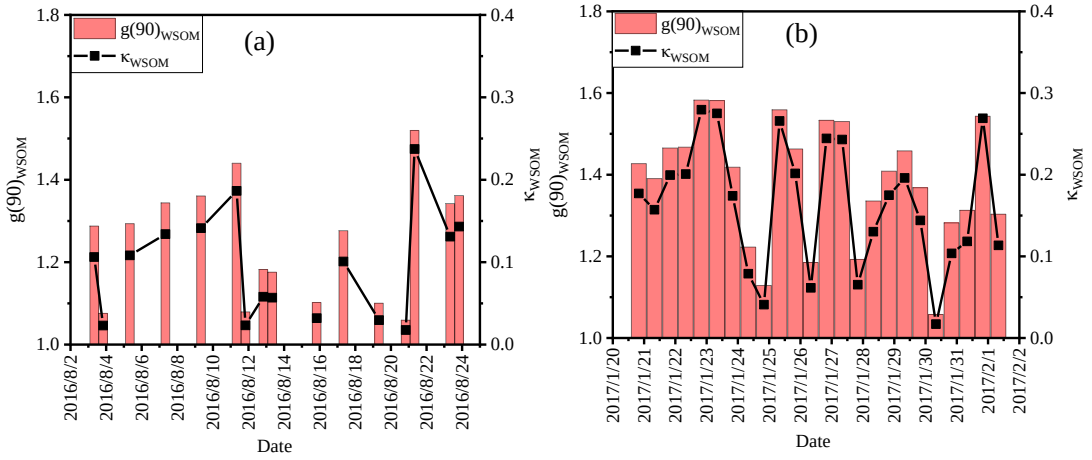

Figure 7 Temporal variations of $g(90\%)_{WSOM}$ and κ_{WSOM} during the study period: (a) for summer, (b) for winter.

The retrieved $g(90\%)_{WSOM}$ and κ for all the samples during the study period is shown in Figure 7. In summer, $g(90\%)_{WSOM}<1$ in some samples, meaning that organic matter does not contribute to the increase of the hygroscopic growth of particles. $g(90\%)_{WSOM}$ ranges from 1.06~1.52 with an average of 1.25±0.14, excluding samples with $g(90\%)_{WSOM}<1$. While in winter, the $g(90\%)_{WSOM}$ of all samples is always greater than 1, in the range of 1.06~1.58 with an average of 1.38±0.15, indicating that organic matters contributes to particle size growth. The corresponding κ values are in the range of 0.02~0.32(0.13±0.09) for summer and 0.02~0.38(0.22±0.10) for winter, respectively. The mean value of $g(90\%)_{WSOM}$ is close to the hygroscopic growth factor of biomass

494 burning indicator, such as levoglucosan (1.29), mannosan (1.28), and galactosan (1.27)
495 (Mikhailov et al., 2009; Michihiro Mochida and Kawamura, 2004b), which adds
496 another evidence for the influence of biomass burning on aerosol particles in the region.
497 More importantly, the correlation between the hygroscopic growth factor of WSOM
498 and the levoglucosan is analyzed to be 0.53 in summer and 0.43 in winter (not shown
499 as figures). This means that levoglucosan contributes only a part to $g(90\%)_{WSOM}$. While
500 in winter heavy haze episode, the hygroscopic growth factor of organics shows a
501 downward trend, indicating that their contribution to particle hygroscopic property
502 decreases. Therefore, it can be inferred that the relative contribution of inorganic
503 substances will increase. This is consistent with the results published in many literatures
504 suggesting that severe haze in winter is caused by an increase in inorganic substances(S
505 K Boreddy et al., 2016; Gysel et al., 2007). However, in non-pollution weather, the
506 hygroscopic growth factor of WSOM increases. When the effects of anthropogenic
507 activities such as severe haze events and New Year's Day were excluded, the correlation
508 parameters(R) of $g(90)_{WSOM}$ and levoglucosan in other weather conditions increased to
509 0.71 (not shown as figures). This further proves that the rural areas in Guanzhong Basin
510 are affected by biomass burning.

511 **4 Conclusion**

512 In this study, we investigated the chemical components and hygroscopic properties
513 of water-soluble fraction in $PM_{2.5}$ aerosols collected from a rural site, Lin village
514 located at Guanzhong Basin. Air pollution in winter over the Guanzhong Basin was a
515 regional problem, not just a local area that needs to be urgently addressed. Inorganic
516 ions predominated the WSM concentration in both seasons, however, the contribution
517 of water-soluble organic matter (WSOM) to WSM increased by 1.4 times from summer
518 to winter. The $g(90)_{WSM}$ values measured by H-TDMA and the retrieved κ_{WSM} was in
519 the range of 1.08~1.49 (1.35±0.10) and 0.04~0.29 (0.190±0.06) in summer, 1.24~1.45
520 (1.36±0.07) and 0.12~0.26 (0.144±0.04) in winter, respectively. $g(90)_{WSM}$ presented fair
521 correlations with levoglucosan, galactosan, and mannosan in winter, suggesting an
522 influence of biomass burning on hygroscopic properties of $PM_{2.5}$ in the region.

Increased nitrate concentration at night in summer reduced the deliquescent point (60%-70%) of the particles, and enhanced the hygroscopic growth factor of the particles at elevated relative humidity. For heavy haze day in winter, SNA are the main components, which greatly contributes to the hygroscopic property of particles (deliquescence point ranges from 50% to 60%). In contrast, more metal matters emitted on Chinese Spring Festival event and WSOM in clean day causes no deliquescence point in the process of hygroscopic growth with the elevated RH. The derived $g(90)_{WSOM}$ and κ_{WSOM} was calculated by ZSR model. The mean value of κ_{WSOM} in this study was significantly lower than that of marine sites and urban sites. The mean $g(90)_{WSOM}$ is in the range of that of biomass burning aerosols. Moreover, it was found that the correlation between $g(90)_{WSOM}$ and levoglucosan increased significantly (R=0.71) after eliminating heavy haze and New Year's events, further confirming the impact of biomass burning in the region.

Acknowledgments, Samples, and Data

This work was financially supported by the Innovation Capability Support Program of Shaanxi (No. 2020KJXX-017), and the program from National Nature Science Foundation of China (No. 41977332). Jianjun Li also acknowledged the support of the Youth Innovation Promotion Association CAS (No. 2020407). The important data supporting the conclusion of the paper are available in the main text. Refer to the data repository website (https://zenodo.org/record/3975821) for more detailed data.

Reference:

Aggarwal, S. G., M. Mochida, Y. Kitamori, & K. Kawamura. (2007). Chemical Closure Study on Hygroscopic Properties of Urban Aerosol Particles in Sapporo, Japan. *Environmental science & technology*, *41*(20), 6920-6925, http://doi.org/10.1021/es063092m

Almeida, G. P., A. T. Bittencourt, M. S. Evangelista, M. S. Vieira-Filho, & A. Fornaro. (2019). Characterization of aerosol chemical composition from urban pollution in Brazil and its possible impacts on the aerosol hygroscopicity and size distribution. *Atmospheric Environment*, *202*, 149-159, http://doi.org/10.1016/j.atmosenv.2019.01.024.

Alonso-Blanco, E., F. J. Gómez-Moreno, & B. Artíñano. (2019). Size-resolved hygroscopicity of ambient

555 submicron particles in a suburban atmosphere. *Atmospheric Environment*, *213*, 349-358,
556 http://doi.org/10.1016/j.atmosenv.2019.05.065.
557 An, J., Q. Cao, J. Zou, H. Wang, Q. Duan, Y. Shi, C. Chen, & J. Wang. (2017). Seasonal Variation in
558 Water-Soluble Ions in Airborne Particulate Deposition in the Suburban Nanjing Area, Yangtze
559 River Delta, China, During Haze Days and Normal Days. *Archives of Environmental*
560 *Contamination and Toxicology*, *74*(1), 1-15, http://doi.org/10.1007/s00244-017-0447-0.
561 Andreae, M. O., & D. J. E. S. R. Rosenfeld. (2008). Aerosol–cloud–precipitation interactions. Part 1. The
562 nature and sources of cloud-active aerosols, *89*(1-2), 13-41,
563 http://doi.org/10.1016/j.earscirev.2008.03.001
564 Bi, X., Y. Feng, J. Wu, Y. Wang, & T. Zhu. (2007). Source apportionment of PM10 in six cities of northern
565 China. *Atmospheric Environment*, *41*(5), 903-912, http://doi.org/10.1016/j.atmosenv.2006.09.033.
566 Boreddy, S. K., & K. Kawamura. (2016). Hygroscopic growth of water-soluble matter extracted from
567 remote marine aerosols over the western North Pacific: Influence of pollutants transported from
568 East Asia. *The Science of the total environment*, *557-558*, 285-295,
569 http://doi.org/10.1016/j.scitotenv.2016.03.096.
570 Boreddy, S. K., K. Kawamura, S. Bikkina, & M. M. Sarin. (2016). Hygroscopic growth of particles
571 nebulized from water-soluble extracts of PM2.5 aerosols over the Bay of Bengal: Influence of
572 heterogeneity in air masses and formation pathways. *The Science of the total environment*, *544*,
573 661-669, http://doi.org/10.1016/j.scitotenv.2015.11.164.
574 Boreddy, S. K. R., K. Kawamura, & J. Jung. (2014). Hygroscopic properties of particles nebulized from
575 water extracts of aerosols collected at Chichijima Island in the western North Pacific: An outflow
576 region of Asian dust. *Journal of Geophysical Research: Atmospheres*, *119*(1), 167-178,
577 http://doi.org/10.1002/2013jd020626.
578 Bouzidi, H., A. Zuend, J. Ondráček, J. Schwarz, & V. Ždímal. (2020). Hygroscopic behavior of
579 inorganic–organic aerosol systems including ammonium sulfate, dicarboxylic acids, and oligomer.
580 *Atmospheric Environment*, *229*, http://doi.org/10.1016/j.atmosenv.2020.117481.
581 Brook, R. D., S. Rajagopalan, C. A. Pope, J. R. Brook, & J. D. Kaufman. (2010). Particulate Matter Air
582 Pollution and Cardiovascular Disease An Update to the Scientific Statement From the American
583 Heart Association. *Circulation*, *121*(21), 2331-2378,
584 http://doi.org/10.1161/CIR.0b013e3181dbece1
585 Calvo, A. I., V. Pont, C. Liousse, B. Dupré, A. Mariscal, C. Zouiten, E. Gardrat, P. Castera, C. G. Lacaux,
586 & A. Castro. (2008). Chemical composition of urban aerosols in Toulouse, France during
587 CAPITOUL experiment. *Meteorology & Atmospheric Physics*, *102*(3-4), 307-323,
588 http://doi.org/10.1007/s00703-008-0319-2
589 Chan, C. K., & X. Yao. (2008). Air pollution in mega cities in China. *Atmos. Environ.*, *42*(1), 1-42,
590 http://doi.org/https://doi.org/10.1016/j.atmosenv.2007.09.003.
591 Chen, S. Y., L. M. Zeng, H. B. Dong, & T. Zhu. (2015). Transformation mechanism and sources of
592 secondary inorganic components in PM2.5 at an agriculture site (Quzhou) in the North China Plain
593 in Summer. *Environmental Science*, *36*(10), 3554.
594 Chen, X.-C., H. J. Jahn, G. Engling, T. J. Ward, A. Kraemer, K.-F. Ho, S. H. L. Yim, & C.-Y. Chan.
595 (2017). Chemical characterization and sources of personal exposure to fine particulate matter
596 (PM2.5) in the megacity of Guangzhou, China. *Environmental pollution*, *231*, 871-881,
597 http://doi.org/https://doi.org/10.1016/j.envpol.2017.08.062.
598 Demott, P. J., M. D. Petters, A. J. Prenni, C. M. Carrico, S. M. Kreidenweis, J. L. C. Jr, & H. J. J. o. G.

R. A. Moosmüller. (2009). Ice nucleation behavior of biomass combustion particles at cirrus temperatures, *114*(D16), -, http://doi.org/10.1029/2009JD012036

Dick, W. D., P. Saxena, & P. H. McMurry. (2000). Estimation of water uptake by organic compounds in submicron aerosols measured during the Southeastern Aerosol and Visibility Study. *Journal of Geophysical Research: Atmospheres*, *105*(D1), 1471-1479, http://doi.org/10.1029/1999jd901001.

Dusek, U., G. P. Frank, J. Curtius, F. Drewnick, & U. Pöschl. (2010a). Enhanced organic mass fraction and decreased hygroscopicity of cloud condensation nuclei (CCN) during new particle formation events. *Geophysical Research Letters*, *37*(3), http://doi.org/10.1029/2009GL040930.

Dusek, U., G. P. Frank, A. Massling, K. Zeromskiene, Y. Iinuma, O. Schmid, G. Helas, T. Hennig, A. Wiedensohler, & M. O. Andreae. (2010b). Water uptake of biomass burning aerosol at sub- and supersaturated conditions: closure studies and implications for the role of organics. *Atmospheric Chemistry and Physics Discussions*, *10*(12), 29853-29895, http://doi.org/10.5194/acpd-10-29853-2010.

Engelhart, G. J., C. J. Hennigan, M. A. Miracolo, A. L. Robinson, & S. N. Pandis. (2012). Cloud condensation nuclei activity of fresh primary and aged biomass burning aerosol. *Atmospheric Chemistry and Physics Discussions*, *12*(3), 7521-7544, http://doi.org/10.5194/acpd-12-7521-2012.

Fernández-Camacho, R., J. D. de la Rosa, & A. M. Sánchez de la Campa. (2016). Trends and sources vs air mass origins in a major city in South-western Europe: Implications for air quality management. *Science of the Total Environment*, *553*, 305-315, http://doi.org/10.1016/j.scitotenv.2016.02.079.

Freney, E. J., S. T. Martin, & P. R. Buseck. (2009). Deliquescence and Efflorescence of Potassium Salts Relevant to Biomass-Burning Aerosol Particles. *Aerosol Science and Technology*, *43*(8), 799-807, http://doi.org/10.1080/02786820902946620.

Gasparini, R., R. Li, & D. R. Collins. (2004). Integration of size distributions and size-resolved hygroscopicity measured during the Houston Supersite for compositional categorization of the aerosol. *Atmospheric Environment*, *38*(20), 3285-3303, http://doi.org/10.1016/j.atmosenv.2004.03.019.

Ge, S., G. Wang, S. Zhang, D. Li, Y. Xie, C. Wu, Q. Yuan, J. Chen, & H. Zhang. (2019). Abundant NH3 in China Enhances Atmospheric HONO Production by Promoting the Heterogeneous Reaction of SO2 with NO2. *Environmental science & technology*, *53*(24), 14339-14347, http://doi.org/10.1021/acs.est.9b04196.

Gysel, M., J. Crosier, D. O. Topping, J. D. Whitehead, K. N. Bower, M. J. Cubison, P. I. Williams, M. J. Flynn, G. B. McFiggans, & H. Coe. (2007). Closure study between chemical composition and hygroscopic growth of aerosol particles during TORCH2. *Atmospheric Chemistry and Physics*, *7*(24), 6131-6144, http://doi.org/10.1007/978-1-4020-6475-3_144

He, B.-J., J. Zhu, D.-X. Zhao, Z. Gou, J. qi, & J. Wang. (2019). Co-benefits approach: Opportunities for implementing sponge city and urban heat island mitigation. *Land Use Policy*, http://doi.org/10.1016/j.landusepol.2019.05.

Hennigan, C. J., J. Izumi, A. P. Sullivan, R. J. Weber, & A. Nenes. (2015). A critical evaluation of proxy methods used to estimate the acidity of atmospheric particles. *Atmospheric Chemistry and Physics*, *15*(5), 2775-2790, http://doi.org/10.5194/acp-15-2775-2015.

Hueglin, C., R. Gehrig, U. Baltensperger, M. Gysel, C. Monn, & H. Vonmont. (2005). Chemical characterisation of PM2.5, PM10 and coarse particles at urban, near-city and rural sites in Switzerland. *Atmospheric Environment*, *39*(4), 637-651, http://doi.org/10.1016/j.atmosenv.2004.10.027.

IPCC (2001), *Climate Change 2001: the scientific basis*, Cambridge University Press, Cambridge, New York, IPCC, 881 pp.

Jin, L., L. Jian-jun, W. Can, C. Cong, W. Yu-hang, L. Lang, H. Jing, & W. Ge-hu. (2018). Comparison on the chemical composition of PM2.5 in the urban and rural regions of Guanzhong plain, China. *China Environmental Science*, *38*(12), 4415~4425, http://doi.org/10.19674/j.cnki.issn1000-6923.2018.0494.

Johannesson, S., P. Gustafson, P. Molnár, L. Barregard, & G. Sallsten. (2007). Exposure to fine particles (PM2.5 and PM1) and black smoke in the general population: personal, indoor, and outdoor levels. *Journal of Exposure Science & Environmental Epidemiology*, *17*(7), 613-624, http://doi.org/10.1038/sj.jes.7500562.

Jung, J., Y. J. Kim, S. G. Aggarwal, & K. Kawamura. (2011). Hygroscopic property of water-soluble organic-enriched aerosols in Ulaanbaatar, Mongolia during the cold winter of 2007. *Atmospheric Environment*, *45*(16), 2722-2729, http://doi.org/10.1016/j.atmosenv.2011.02.055.

Junji, C., S. Zhenxing, C. C. Judith, Q. Guowei, & G. W. John. (2009). Seasonal variations and sources of mass and chemical composition for PM10 aerosol in Hangzhou, China. *China Particuology*, *7*(3), 161-168, http://doi.org/10.1016/j.partic.2009.01.009.

Karagulian, F., C. A. Belis, C. F. C. Dora, A. M. Prüss-Ustün, S. Bonjour, H. Adair-Rohani, & M. Amann. (2015). Contributions to cities' ambient particulate matter (PM): A systematic review of local source contributions at global level. *Atmospheric Environment*, *120*, 475-483, http://doi.org/10.1016/j.atmosenv.2015.08.087.

Kotchenruther, R. A., & P. V. J. J. o. G. R. A. Hobbs. (1998). Humidification factors of aerosols from biomass burning in Brazil. *JOURNAL OF GEOPHYSICAL RESEARCH*, *103*(D24), 32081-32089, http://doi.org/10.1029/98JD00340.

Kreidenweis, S. M., & A. J. T. o. G. Asa-Awuku. (2014). Aerosol Hygroscopicity: Particle Water Content and Its Role in Atmospheric Processes. *Treatise on Geochemistry*, *5*, 331-361, http://doi.org/10.1016/B978-0-08-095975-7.00418-6

Lee, W. M., W. M. Huang, & Y. Y. Chen. (2001). Effect of relative humidity on mixed aerosols in atmosphere. *J Environ Sci Health A Tox Hazard Subst Environ Eng*, *36*(4), 533-544, http://doi.org/10.1081/ese-100103482.

Li, C., Y. Hu, J. Chen, Z. Ma, X. Ye, X. Yang, L. Wang, X. Wang, & A. Mellouki. (2016). Physiochemical properties of carbonaceous aerosol from agricultural residue burning: Density, volatility, and hygroscopicity. *Atmospheric Environment*, *140*, 94-105, http://doi.org/10.1016/j.atmosenv.2016.05.052.

Li, J., G. Wang, S. G. Aggarwal, Y. Huang, Y. Ren, B. Zhou, K. Singh, P. K. Gupta, J. Cao, & R. Zhang. (2014). Comparison of abundances, compositions and sources of elements, inorganic ions and organic compounds in atmospheric aerosols from Xi'an and New Delhi, two megacities in China and India. *The Science of the total environment*, *476-477*, 485-495, http://doi.org/10.1016/j.scitotenv.2014.01.011.

Li, J., G. Wang, B. Zhou, C. Cheng, J. Cao, Z. Shen, & Z. An. (2011). Chemical composition and size distribution of wintertime aerosols in the atmosphere of Mt. Hua in central China. *Atmospheric Environment*, *45*(6), 1251-1258, http://doi.org/10.1016/j.atmosenv.2010.12.009.

Li, J., et al. (2020). Optical properties and molecular compositions of water-soluble and waterinsoluble brown carbon (BrC) aerosols in Northwest China. *Atmos. Chem. Phys.*,, *20*(8), 4889-4904, http://doi.org/10.5194/acp-2019-1002.

687 Liu, H. J., C. S. Zhao, B. Nekat, N. Ma, A. Wiedensohler, D. van Pinxteren, G. Spindler, K. Müller, &
688 H. Herrmann. (2014a). Aerosol hygroscopicity derived from size-segregated chemical composition
689 and its parameterization in the North China Plain. *Atmospheric Chemistry and Physics*, *14*(5),
690 2525-2539, http://doi.org/10.5194/acp-14-2525-2014.
691 Liu, Q., B. Jing, C. Peng, S. Tong, W. Wang, & M. Ge. (2016a). Hygroscopicity of internally mixed
692 multi-component aerosol particles of atmospheric relevance. *Atmospheric Environment*, *125*, 69-
693 77, http://doi.org/10.1016/j.atmosenv.2015.11.003.
694 Liu, X. G., Y. H. Zhang, M. T. Wen, J. L. Wang, J. Jung, S. Y. Chang, M. Hu, L. M. Zeng, & Y. J. Kim.
695 (2010). A closure study of aerosol hygroscopic growth factor during the 2006 Pearl River Delta
696 Campaign. *Advances in Atmospheric Sciences*, *27*(4), 947-956, http://doi.org/10.1007/s00376-009-
697 9150-z.
698 Liu, Y., Z. Wu, T. Tan, Y. Wang, Y. Qin, J. Zheng, M. Li, & M. Hu. (2016b). Estimation of the PM2.5
699 effective hygroscopic parameter and water content based on particle chemical composition:
700 Methodology and case study. *Science China Earth Sciences*, *59*(8), 1683-1691,
701 http://doi.org/10.1007/s11430-016-5313-9.
702 Liu, Z., B. Hu, L. Wang, F. Wu, W. Gao, & Y. Wang. (2014b). Seasonal and diurnal variation in particulate
703 matter (PM10 and PM2.5) at an urban site of Beijing: analyses from a 9-year study. *Environmental*
704 *Science and Pollution Research*, *22*(1), 627-642, http://doi.org/10.1007/s11356-014-3347-0.
705 Luo, Q., J. Hong, H. Xu, S. Han, H. Tan, Q. Wang, J. Tao, N. Ma, Y. Cheng, & H. Su. (2020).
706 Hygroscopicity of amino acids and their effect on the water uptake of ammonium sulfate in the
707 mixed aerosol particles. *The Science of the total environment*, *734*, 139318,
708 http://doi.org/10.1016/j.scitotenv.2020.139318.
709 Ma, J., X. Xu, C. Zhao, & P. Yan. (2012). A review of atmospheric chemistry research in China:
710 Photochemical smog, haze pollution, and gas-aerosol interactions. *Advances in Atmospheric*
711 *Sciences*, *29*(5), 1006-1026, http://doi.org/10.1007/s00376-012-1188-7.
712 Magi, B. I., & P. V. Hobbs. (2003). Effects of humidity on aerosols in southern Africa during the biomass
713 burning season. *J Geophys Res-Atmos*, *108*(D13), 8495, http://doi.org/10.1029/2002jd002144.
714 Meyer, N. K., et al. (2008). Analysis of the hygroscopic and volatile properties of ammonium sulphate
715 seeded and unseeded SOA particles. *Atmospheric Chemistry and Physics*, *9*(2), 721-732
716 http://doi.org/10.5194/acp-9-721-2009.
717 Mikhailov, E., S. Vlasenko, S. T. Martin, T. Koop, & U. Poschl. (2009). Amorphous and crystalline
718 aerosol particles interacting with water vapor: conceptual framework and experimental evidence
719 for restructuring, phase transitions and kinetic limitations. *Atmospheric Chemistry And Physics*,
720 *9*(24), 9491-9522, http://doi.org/DOI 10.5194/acp-9-9491-2009.
721 Mochida, M., & K. Kawamura. (2004a). Hygroscopic properties of levoglucosan and related organic
722 compounds characteristic to biomass burning aerosol particles. *J Geophys Res-Atmos*, *109*(D21),
723 n/a-n/a, http://doi.org/10.1029/2004jd004962.
724 Mochida, M., & K. Kawamura. (2004b). Hygroscopic properties of levoglucosan and related organic
725 compounds characteristic to biomass burning aerosol particles. *Journal of Geophysical Research:*
726 *Atmospheres*, *109*(D21), n/a-n/a, http://doi.org/10.1029/2004jd004962.
727 Paraskevopoulou, D., E. Liakakou, E. Gerasopoulos, & N. Mihalopoulos. (2015). Sources of atmospheric
728 aerosol from long-term measurements (5years) of chemical composition in Athens, Greece. *Science*
729 *of The Total Environment*, *527-528*, 165-178, http://doi.org/10.1016/j.scitotenv.2015.04.022.
730 Petrowski, K., C. D. Bastianon, S. Bührer, & E. Brähler. (2019). Air quality and chronic stress: A

representative study of air pollution (PM2.5, PM10) in Germany. *Journal of Occupational and Environmental Medicine*, *61*(2), 144-147, http://doi.org/10.1097/jom.0000000000001502.

Petters, M. D., & S. M. Kreidenweis. (2007). A single parameter representation of hygroscopic growth and cloud condensation nucleus activity. *Atmospheric Chemistry and Physics*, *7*(8), 1961-1971, http://doi.org/10.5194/acp-7-1961-2007.

Psichoudaki, M., A. Nenes, K. Florou, C. Kaltsonoudis, & S. N. J. A. E. Pandis. (2018). Hygroscopic properties of atmospheric particles emitted during wintertime biomass burning episodes in Athens, *178*(APR.), 66-72, http://doi.org/10.1016/j.atmosenv.2018.01.004.

Rose, D., A. Nowak, P. Achtert, A. Wiedensohler, M. Hu, M. Shao, Y. Zhang, M. O. Andreae, & U. Pöschl. (2010). Cloud condensation nuclei in polluted air and biomass burning smoke near the mega-city Guangzhou, China – Part 1: Size-resolved measurements and implications for the modeling of aerosol particle hygroscopicity and CCN activity. *Atmospheric Chemistry and Physics*, *10*(7), 3365-3383, http://doi.org/10.5194/acp-10-3365-2010.

Schaap, M., M. van Loon, H. M. ten Brink, F. J. Dentener, & P. J. H. Builtjes. (2004). Secondary inorganic aerosol simulations for Europe with special attention to nitrate. *Atmospheric Chemistry and Physics*, *4*(3), 857-874, http://doi.org/10.5194/acp-4-857-2004

Shen, Z., J. Cao, L. Zhang, L. Liu, Q. Zhang, J. Li, Y. Han, C. Zhu, Z. Zhao, & S. Liu. (2014). Day–night differences and seasonal variations of chemical species in PM10over Xi'an, northwest China. *Environ Sci Pollut Res Int*, *21*(5), 3697-3705, http://doi.org/10.1007/s11356-013-2352-z.

Steven, H., S. Hang, X. Hongmei, H. Rujin, & C. Junji. (2016). PM2.5 from the Guanzhong Plain: Chemical composition and implications for emission reductions. *Atmospheric Environment*, *147*, 458-469, http://doi.org/10.1016/j.atmosenv.2016.10.029

Sun, J., et al. (2019). Effects of biomass briquetting and carbonization on PM2.5 emission from residential burning in Guanzhong Plain, China. *Fuel*, *244*, 379-387, http://doi.org/10.1016/j.fuel.2019.02.031.

Suresh Kumar Reddy, B., K. Kawamura, S. L. Mkoma, & P. Fu. (2014). Hygroscopic behavior of water-soluble matter extracted from biomass burning aerosols collected at a rural site in Tanzania, East Africa. *Journal of Geophysical Research*, *119*, 12233-12245, http://doi.org/10.1002/2014JD021546.

Swietlicki, E., et al. (2017). Hygroscopic properties of submicrometer atmospheric aerosol particles measured with H-TDMA instruments in various environments—a review. *Tellus B: Chemical and Physical Meteorology*, *60*(3), 432-469, http://doi.org/10.1111/j.1600-0889.2008.00350.x.

Tang, M., et al. (2019). A review of experimental techniques for aerosol hygroscopicity studies. *Atmospheric Chemistry and Physics*, *19*(19), 12631-12686, http://doi.org/10.5194/acp-19-12631-2019.

van Donkelaar, A., R. V. Martin, M. Brauer, R. Kahn, R. Levy, C. Verduzco, & P. J. Villeneuve. (2010). Global estimates of ambient fine particulate matter concentrations from satellite-based aerosol optical depth: development and application. *Environmental health perspectives*, *118*(6), 847-855, http://doi.org/10.1289/ehp.0901623.

Wang, G., et al. (2018a). Particle acidity and sulfate production during severe haze events in China cannot be reliably inferred by assuming a mixture of inorganic salts. *Atmospheric Chemistry and Physics*, *18*(14), 10123-10132, http://doi.org/10.5194/acp-18-10123-2018.

Wang, G., et al. (2016a). Persistent sulfate formation from London Fog to Chinese haze. *Proceedings of the National Academy of Sciences*, *113*(48), 13630-13635, http://doi.org/10.1073/pnas.1616540113.

Wang, J., S. Lai, Z. Ke, Y. Zhang, S. Yin, & J. Zheng. (2013). Exposure assessment, chemical characterization and source identification of PM2.5 for school children and industrial downwind residents in Guangzhou, China. *Environmental Geochemistry and Health*, *36*(3), 385-397, http://doi.org/10.1007/s10653-013-9557-4.

Wang, S., G. Li, Z. Gong, L. Du, Q. Zhou, X. Meng, S. Xie, & L. Zhou. (2015). Spatial distribution, seasonal variation and regionalization of PM2.5 concentrations in China. *Science China Chemistry*, *58*(9), 1435-1443, http://doi.org/10.1007/s11426-015-5468-9.

Wang, T. J., F. Jiang, J. J. Deng, Y. Shen, Q. Y. Fu, Q. Wang, Y. Fu, J. H. Xu, & D. N. Zhang. (2012). Urban air quality and regional haze weather forecast for Yangtze River Delta region. *Atmospheric Environment*, *58*, 70-83, http://doi.org/10.1016/j.atmosenv.2012.01.014.

Wang, X., X. J. Shen, J. Y. Sun, X. Y. Zhang, Y. Q. Wang, Y. M. Zhang, P. Wang, C. Xia, X. F. Qi, & J. T. Zhong. (2018b). Size-resolved hygroscopic behavior of atmospheric aerosols during heavy aerosol pollution episodes in Beijing in December 2016. *Atmospheric Environment*, *194*, 188-197, http://doi.org/10.1016/j.atmosenv.2018.09.041.

Wang, Y., B. Jing, Y. Guo, J. Li, S. Tong, Y. Zhang, & M. Ge. (2016b). Water uptake of multicomponent organic mixtures and their influence on hygroscopicity of inorganic salts. *Journal of environmental sciences*, *45*, 156-163, http://doi.org/10.1016/j.jes.2016.01.013.

Wang, Z., B. Jing, X. Shi, S. Tong, W. Wang, & M. Ge. (2018c). Importance of water-soluble organic acid on the hygroscopicity of nitrate. *Atmospheric Environment*, *190*, 65-73, http://doi.org/10.1016/j.atmosenv.2018.07.010.

Wexler, A. S., & J. H. Seinfeld. (1991). Second-generation inorganic aerosol model. *Atmospheric Environment*, *25*(12), 2731-2748, http://doi.org/10.1016/0960-1686(91)90203-J

Wu, Y., X. Wang, P. Yan, L. Zhang, J. Tao, X. Liu, P. Tian, Z. Han, & R. Zhang. (2017a). Investigation of hygroscopic growth effect on aerosol scattering coefficient at a rural site in the southern North China Plain. *The Science of the total environment*, *599-600*, 76-84, http://doi.org/10.1016/j.scitotenv.2017.04.194.

Wu, Z., J. Zheng, Y. Wang, D. Shang, Z. Du, Y. Zhang, & M. Hu. (2017b). Chemical and physical properties of biomass burning aerosols and their CCN activity: A case study in Beijing, China. *The Science of the total environment*, *579*, 1260-1268, http://doi.org/10.1016/j.scitotenv.2016.11.112.

Wu, Z. J., J. Zheng, D. J. Shang, Z. F. Du, & M. Hu. (2015). Particle hygroscopicity and its link to chemical composition in the urban atmosphere of Beijing, China during summertime. *Atmospheric Chemistry & Physics*, *15*(8), 11495-11524, http://doi.org/10.5194/acpd-15-11495-2015

Xiang, P., X. Zhou, J. Duan, J. Tan, & Y. Zhang. (2016). Chemical characteristics of water-soluble organic compounds (WSOC) in PM2.5 in Beijing, China: 2011–2012. *Atmospheric Research*, *183*, 104-112, http://doi.org/10.1016/j.atmosres.2016.08.020.

Xie, Y., et al. (2020). Nitrate-dominated PM_{2.5} and elevation of particle pH observed in urban Beijing during the winter of 2017. *Atmospheric Chemistry and Physics*, *20*(8), 5019-5033, http://doi.org/10.5194/acp-20-5019-2020.

Xu, H., et al. (2018). Personal exposure of PM2.5 emitted from solid fuels combustion for household heating and cooking in rural Guanzhong Plain, northwestern China. *Atmospheric Environment*, *185*, 196-206, http://doi.org/10.1016/j.atmosenv.2018.05.018.

Xu, H., Z. Xiao, K. Chen, M. Tang, N. Zheng, P. Li, N. Yang, W. Yang, & X. Deng. (2019). Spatial and temporal distribution, chemical characteristics, and sources of ambient particulate matter in the Beijing-Tianjin-Hebei region. *The Science of the total environment*, *658*, 280-293,

http://doi.org/10.1016/j.scitotenv.2018.12.164.

Yan, Y., P. Fu, B. Jing, C. Peng, S. K. Boreddy, F. Yang, L. Wei, Y. Sun, Z. Wang, & M. Ge. (2017). Hygroscopic behavior of water-soluble matter in marine aerosols over the East China Sea. *The Science of the total environment*, *578*, 307-316, http://doi.org/10.1016/j.scitotenv.2016.10.149.

Yao, H., W. Ge-hui, R. Yan-qing, H. Yan-ni, C. Yu-bao, C. Chun-lei, W. Jia-yuan, & L. Jian-jun. (2015). Hourly characteristic of chemical composition and hygroscopic property of TSP in Xi'an during dust storm. *Journal of Earth Environment*, *6*(28 (01)), 48-57, http://doi.org/10.7515/JEE20150100*.

Yao, L., & N. Lu. (2014). Spatiotemporal distribution and short-term trends of particulate matter concentration over China, 2006–2010. *Environmental Science and Pollution Research*, *21*(16), 9665-9675, http://doi.org/10.1007/s11356-014-2996-3.

Ye, X., C. Tang, Z. Yin, J. Chen, Z. Ma, L. Kong, X. Yang, W. Gao, & F. Geng. (2013). Hygroscopic growth of urban aerosol particles during the 2009 Mirage-Shanghai Campaign. *Atmospheric Environment*, *64*, 263-269, http://doi.org/10.1016/j.atmosenv.2012.09.064.

Yu, K., et al. (2018). Association of Solid Fuel Use With Risk of Cardiovascular and All-Cause Mortality in Rural China. *Jama*, *319*(13), 1351-1361, http://doi.org/10.1001/jama.2018.2151.

Yue, D. L., L. J. Zhong, T. Zhang, J. Shen, Y. Zhou, L. M. Zeng, H. B. Dong, & S. Q. Ye. (2015). Pollution Properties of Water-Soluble Secondary Inorganic Ions in Atmospheric PM_(2.5) in the Pearl River Delta Region. *Aerosol & Air Quality Research*, *15*(5), 1737-1747, http://doi.org/10.4209/aaqr.2014.12.0333

Zhang, J. C., L. Wang, J. M. Chen, S. M. Feng, J. D. Shen, & L. Jiao. (2011a). Hygroscopicity of ambient submicron particles in urban Hangzhou, China. *Frontiers of Environmental Science & Engineering in China*, *5*(3), 342-347, http://doi.org/10.1007/s11783-011-0358-7.

Zhang, T., et al. (2011b). Water-soluble ions in atmospheric aerosols measured in Xi'an, China: Seasonal variations and sources. *Atmospheric Research*, *102*(1-2), 110-119, http://doi.org/10.1016/j.atmosres.2011.06.014.

Zhang, X., X. Xu, Y. Ding, Y. Liu, H. Zhang, Y. Wang, & J. Zhong. (2019). The impact of meteorological changes from 2013 to 2017 on PM2.5 mass reduction in key regions in China. *Science China Earth Sciences*, *62*(12), 1885-1902, http://doi.org/10.1007/s11430-019-9343-3.

Zhao, Z.-Q., B.-J. He, L.-G. Li, H.-B. Wang, & A. Darko. (2017). Profile and concentric zonal analysis of relationships between land use/land cover and land surface temperature: Case study of Shenyang, China. *Energy and Buildings*, *155*, 282-295, http://doi.org/10.1016/j.enbuild.2017.09.046.